⌘ *Author's Choice*

THE JOURNAL OF BIOLOGICAL CHEMISTRY VOL. 288, NO. 5, pp. 3641–3654, February 1, 2013

Accelerated Disease Onset with Stabilized Familial Amyotrophic Lateral Sclerosis (ALS)-linked Mutant TDP-43 Proteins*

Received for publication, November 4, 2012, and in revised form, December 10, 2012 Published, JBC Papers in Press, December 12, 2012, DOI 10.1074/jbc.M112.433615

Shoji Watanabe[‡§], **Kumi Kaneko**[‡], **and Koji Yamanaka**[‡¶‖**1]

From the [‡]*Laboratory for Motor Neuron Disease, RIKEN Brain Science Institute, Wako, Saitama 351-0198, the* [§]*Graduate School of Brain Science, Doshisha University, Kizugawa, Kyoto, 619-0225, the* [¶]*Japan Science and Technology Agency, CREST, Saitama 332-0012, the* [‖]*Brain Science Institute, Saitama University, Saitama, 338-8570, and the* [**]*Graduate School of Medicine, Kyoto University, 606-8501 Kyoto, Japan*

Background: Dominant mutations in TDP-43 cause familial ALS.
Results: Longer half-lives of mutant TDP-43 proteins correlated with earlier disease onset, and stabilized TDP-43 provoked protein insolubility, cleavage, RNA dysregulation, and cytotoxicity.
Conclusion: Increased stability of TDP-43 causes toxicity through abnormal proteostasis and RNA dysregulation.
Significance: This is the first TDP-43 cell model based on genotype-phenotype correlation of ALS patients.

Abnormal protein accumulation is a pathological hallmark of neurodegenerative diseases, including accumulation of TAR DNA-binding protein 43 (TDP-43) in amyotrophic lateral sclerosis (ALS). Dominant mutations in the *TDP-43* gene are causative for familial ALS; however, the relationship between mutant protein biochemical phenotypes and disease course and their significance to disease pathomechanism are not known. Here, we found that longer half-lives of mutant proteins correlated with accelerated disease onset. Based on our findings, we established a cell model in which chronic stabilization of wild-type TDP-43 protein provoked cytotoxicity and recapitulated pathogenic protein cleavage and insolubility to the detergent Sarkosyl, TDP-43 properties that have been observed in sporadic ALS lesions. Furthermore, these cells showed proteasomal impairment and dysregulation of their own mRNA levels. These results suggest that chronically increased stability of mutant or wild-type TDP-43 proteins results in a gain of toxicity through abnormal proteostasis.

Abnormal accumulation of TDP-43[2] has been identified as a pathological hallmark of both ALS and frontotemporal lobar degeneration (1, 2). TDP-43-positive protein inclusions have also been found in other neurodegenerative diseases, including Alzheimer and Parkinson diseases. These findings have led to the concept of TDP-43 proteinopathy, in which nuclear TDP-43 is sequestered and accumulates in the cytoplasm of neurons and glial cells in those neurodegenerative conditions (3, 4). Although there is a wide spectrum of TDP-43-linked diseases, more than 30 mutations in *TDP-43* have been identified in familial and sporadic ALS, indicating that TDP-43 dysfunction through those mutations is somewhat specific to ALS pathogenesis (3, 5–7).

TDP-43 is a ubiquitously expressed DNA- and RNA-binding nuclear protein, and it plays multiple roles in RNA metabolism, including pre-mRNA splicing, translational control, and regulation of mRNA stability (8). Notably, TDP-43 has been shown to control its own mRNA stability through direct binding of TDP-43 protein (9, 10), indicating that the expression level of TDP-43 protein is tightly regulated. In mice, overexpression of wild-type TDP-43 provokes neurodegeneration (11–14), and elimination of TDP-43 leads to early embryonic lethality (15–17). However, the mechanisms by which TDP-43 dysfunction contributes to neurodegeneration have not yet been elucidated. The key unresolved questions in understanding ALS pathomechanisms are whether ALS-causing TDP-43 mutant proteins have different properties from the wild-type protein and, if so, what these mutant properties are.

Full-length TDP-43 and the C-terminal portion carrying ALS-causing mutations show an increased propensity for aggregation in yeast (18) and mammalian cells (19, 20). GFP-fused TDP-A315T protein shows an increased tendency to mislocalize to the cytoplasm and produce higher toxicity to primary neurons than wild-type TDP-43 (21). In terms of protein stability, three ALS-linked mutant proteins were found to have longer half-lives than wild-type TDP-43 in non-neuronal cells (22). Because mice overexpressing either wild-type or ALS-linked mutant TDP-43 transgenes under authentic or heterologous promoters have exhibited varying degrees of motor impairment or neurodegeneration, whether TDP-43 toxicity is substantially enhanced by the ALS-related mutations remains unclear (4, 23). Furthermore, there is accumulating clinical information from familial ALS patients with TDP-43 mutations. However, whether the ages of disease onset or the dura-

* This work was supported by Grants-in-aid for Scientific Research on Innovative Areas 23111006 and 23110523 (to K. Y.) and 22700404 (to S. W.) for Young Scientists (B) from the Ministry for Education, Culture, and Sports, Science and Technology of Japan, grants-in-aid from the Research Committee of CNS Degenerative Diseases, the Ministry of Health, Labour, and Welfare of Japan, The Takeda Science Foundation, and The Naito Foundation (to K. Y.).
⌘ *Author's Choice*—Final version full access.
[1] To whom correspondence should be addressed: Laboratory for Motor Neuron Disease, RIKEN Brain Science Institute, 2-1 Hirosawa, Wako-shi, Saitama, 351-0198, Japan. Tel.: 81-48-467-9677; Fax: 81-48-467-9725; E-mail: kyamanaka@brain.riken.jp.
[2] The abbreviations used are: TDP-43, TAR DNA-binding protein-43; ALS, amyotrophic lateral sclerosis; AHA, L-azidohomoalanine; DD, destabilizing domain of FK-binding protein; PI, propidium iodide; NES, nuclear export signal; NLS, nuclear localization signal; h, human; CFTR, cystic fibrosis transmembrane regulator; Bt_2cAMP, dibutyryl cyclic AMP.

tion of familial ALS patients and the biochemical properties of mutant TDP-43 proteins are correlated is also unknown.

In this study, we aimed to identify biochemical properties that are common to disease-causing TDP-43 mutations and correlated with the age of onset or disease progression. We found that longer half-lives of mutant proteins correlated with accelerated disease onset. Based on this finding, we established a new cell model in which increased stability of wild-type TDP-43 proteins provoked dysregulation of *TDP-43* mRNA and impaired proteasome activity and cytotoxicity. Furthermore, our cell models recapitulated TDP-43 properties that have been observed in sporadic ALS as follows: protein cleavage and insolubility to the detergent Sarkosyl (1, 2). These findings suggest that chronically increased stability of mutant TDP-43 protein leads to neurodegeneration in familial TDP-43-linked ALS.

EXPERIMENTAL PROCEDURES

Construction of Human TDP-43 and Other Expression Vectors—Human TDP-43 (hTDP-43) DNA fragment was amplified using a HEK293 cDNA library with a pair of oligonucleotides (forward, 5′-*NNNN*GCGATCGCCACCATGTCTGAATATATTCGGGTAACCGAA-3′, and reverse, 5′-*NNNN*GTTTAAACCTACATTCCCCAGCCAGAAGACTTAGAATCC-3′, where *N* represents the four-nucleotide mixture, and underlines indicate SgfI and PmeI sites, respectively), and cloned into the SgfI-PmeI site of the mammalian expression vector pF5K CMV-neo Flexi (Promega) to generate pF5K-hTDP-43. Familial ALS-linked mutations were introduced by site-directed mutagenesis. The mutants of NLS (NLS1/2) and NES (NES1/2) were generated by the same method as above, resulting in TDP-43$^{K82A/R83A/K84A/K95A/K97A/R98A}$ (ΔNLS1/2) and TDP-43$^{I239A/L243A/L248A/I249A/I250A}$ (ΔNES1/2) (24).

To measure the exon skipping activity of hTDP-43, pF5K-hCFTR exon9 was constructed with modification of pTG11T5-hCFTR exon9 (a gift from Dr. Francisco Baralle, International Centre for Genetic Engineering and Biotechnology, Italy) (25, 26). A DNA fragment covering an entire mini-gene, including CFTR exon9, was amplified with pTG11T5-hCFTR exon9 as template and a synthetic oligonucleotides pair (forward, 5′-*NNNN*GCGATCGCCACCATGTTCCTGTCCTTCCCCACCACCAAG-3′, and reverse, 5′-*NNNN*GTTTAAACTTTATTGGCCACCGAGGCTCCAGCTTAACG-3′, where *N* indicates the four nucleotides mixture, and underlines indicate SgfI and PmeI sites, respectively). Amplified DNA fragment was purified and cloned into SgfI-PmeI site of pF5K CMV-neo Flexi.

To construct the FK-binding protein-destabilized domain (DD)-fused hTDP-43 expression vector (DD-hTDP-43), the hTDP-43 fragment was amplified by pF5K-hTDP-43 as a template and synthetic oligonucleotides pair (forward, 5′-GGACTCAGATCTCGAGcttctgaatatattcgggtaaccgaag-3′, and reverse, 5′-TCTAGAGTCGCGGCCGCctacattccccagccagaagact-3′, where capital letters indicate a linker sequence for In-Fusion reaction (Clontech)). The amplified fragment was purified and introduced to the XhoI and NotI site of pPtuner-IRES2 (Clontech) through In-Fusion reaction according to the manufacturer's procedure. To visualize DD-fused hTDP-43, a DD-mCherry-fused hTDP-43 expression vector was constructed. Human TDP-43 fragment was amplified with pF5K-hTDP-43 as a template and the oligonucleotide pair (forward, 5′-CGGGGTACCTCTGAATATATTCGGGTAACCGAAG-ATG-3′, and reverse, 5′-CGCGGATCCCTACATTCCCCAG-CCAGAAGACTTAGAATCCA-3′, where underlines represent KpnI and BamHI sites, respectively). The amplified fragment was purified and inserted into KpnI and BamHI sites of pmCherry-C1. The mCherry-fused TDP-43 fragment was amplified with pmCherry-hTDP-43 as a template and a pair of oligonucleotides (forward, 5′-GGACTCAGATCTCGAGctgt-gagcaagggcgaggaggataaca-3′, and reverse, 5′-TCTAGAGTCG-CGGCCGCctacattccccagccagaagact-3′, where capital letters indicate a linker sequence for In-Fusion reaction). Amplified fragment was purified and cloned into XhoI and NotI site of pPtuner-IRES with In-Fusion reaction.

The Ub^{G76V}-AcGFP vector to monitor proteasome activity (27) was generated as follows. Human ubiquitin fragment was amplified by the HEK293 cDNA library and synthetic oligonucleotides pair (forward, 5′-CTAGCTAGCTAGCG-CCACCATGCAGATTTTCGTG-3′, and reverse, 5′-CCG-CTCGAG**CTTACCCTTACCCTTACCTACTAC**ACCAC-GAAGTCTCAACACAAGATGAAGAGTAGACTC-3′, where underlines indicate NheI and XhoI sites, respectively, and *boldface letters* indicate mutation in human ubiquitin and linker sequence for effective degradation). DNA fragment was purified and cloned into NheI and XhoI sites of pAcGFP-N1 (Clontech).

Reagents and Antibodies—Reagents were obtained from the following suppliers: Shield1 (Clontech); MG132 (Peptide Institute Inc., Japan); wortmannin, rapamycin, and bafilomycin A1 (Sigma). The following antibodies were used for this study: anti-human TDP-43 monoclonal antibody (2E2-D3; Abnova, Taiwan); anti-GAPDH monoclonal antibody (Millipore); anti-AcGFP monoclonal antibody (Clontech); anti-TDP-43 C-terminal polyclonal antibody (Cosmo Bio Co. Ltd., Japan); anti-p62/SQSTM polyclonal antibody (MBL, Japan), and anti-LC3 polyclonal antibody (MBL).

Cell Culture and Transfection—Neuro2a cells were grown in DMEM (Invitrogen) supplemented with 10% FBS (Invitrogen), 100 units/ml penicillin G, and 100 μg/ml streptomycin (Invitrogen). For chemical pulse-chase experiments, methionine- and cysteine-free DMEM was supplemented with 0.2 mM L-cysteine-2HCl (Sigma), 1 mM sodium pyruvate (Invitrogen), GlutaMAX™ (Invitrogen), and dialyzed fetal bovine serum (FBS). Neuro2a cells were transiently transfected with Lipofectamine™ 2000 or Lipofectamine™ LTX (Invitrogen) according to the manufacturer's protocol. Transfected Neuro2a cells were differentiated in all experiments using the following protocol unless otherwise indicated. Four to 6 h after transfection, the culture medium was replaced with fresh advanced DMEM/F12-GlutaMAX (Invitrogen) containing 1% FBS and 2.5 mM Bt_2cAMP (dibutyryl cyclic AMP, Nacalai Tesque, Japan), and cells were further incubated for 24 h to induce differentiation (28).

Immunoblotting—Protein samples were separated by a 5–20% gradient gel (ATTO, Japan) electrophoresis and transferred to PVDF membranes (Millipore). Membranes were blocked with 2% bovine serum albumin (BSA) in phosphate-

buffered saline (PBS) and then incubated with primary antibody in PBS containing 1% BSA and 0.1% Tween 20, followed by incubation with horseradish peroxidase (HRP)-conjugated secondary antibody (GE Healthcare). Membranes were visualized with SuperSignal West Dura Extended Duration Substrate (Thermo Scientific) according to the manufacturer's instructions.

Pulse-Chase Assay by Chemical Labeling of Newly Synthesized Proteins—Newly synthesized proteins were chemically labeled by a click reaction. Neuro2a cells (6×10^5 cells) in 6-well plates were transiently transfected with 2 μg of DNA and Lipofectamine^{TM} 2000. After 4 h of incubation, cells were differentiated with 2.5 mM Bt_2cAMP for 12 h and then incubated with dialyzed FBS- and methionine-free DMEM supplemented with 2.5 mM Bt_2cAMP for 10 h to eliminate intracellular methionine. Newly synthesized proteins were pulse-labeled with a methionine analog, AHA (L-azidohomoalanine, Invitrogen), for 4 h, followed by an arbitrary time chase with DMEM/F-12 GlutaMAX^{TM} medium (Invitrogen) supplemented with 10% FBS and 2.5 mM Bt_2cAMP. After pulse-chase labeling, cells were lysed using 50 μl of 50 mM Tris-HCl (pH 8.0), 1% SDS, 20 units of benzonase (Novagen), and 2× complete protease inhibitor (Roche Applied Science). The cell lysate was boiled for 5 min and then centrifuged at 15,000 × *g* for 5 min to eliminate cell debris. This clear lysate was reacted with biotin alkyne (PEG4 carboxamide-propargyl biotin, Invitrogen) in the presence of $CuSO_4$ for 20 min at room temperature. In this reaction, AHA-labeled proteins were modified by PEG-biotin through the azo group. To terminate this reaction, proteins were precipitated using methanol/chloroform. Following immunoprecipitation using an anti-TDP-43 C-terminal antibody under denaturing conditions, AHA-labeled TDP-43 protein was visualized by high affinity HRP-conjugated streptavidin (Thermo Scientific).

Immunoprecipitation under Denaturing Conditions—Immunoprecipitation under denaturing conditions was carried out as described previously (29). Briefly, a protein sample precipitated by methanol/chloroform was diluted with 1 ml of buffer containing 50 mM Tris-HCl (pH 7.5), 150 mM NaCl, 2% Triton X-100, 1 mM EDTA, and 2× complete protease inhibitor. An antibody directed against the TDP-43 C terminus was added to the resultant supernatant, and the mixture was incubated for 18 h at 4 °C. Protein G-Sepharose (30 μl, GE Healthcare) was added, and then the sample was gently mixed for 60 min at room temperature. After centrifugation at 700 × *g* for 1 min, the resultant pellets were sequentially washed with 0.5 ml of 50 mM Tris-HCl (pH 7.5), 150 mM NaCl, and 1% Triton X-100 followed by 0.5 ml of 50 mM Tris-HCl (pH 7.5), 0.5 M NaCl, and 0.05% SDS. The washed protein G-Sepharose was resuspended in 30 μl of SDS sample buffer and then boiled for 5 min. This sample was centrifuged at 1,000 × *g* for 5 min, and the resultant supernatant was then separated by SDS-PAGE. AHA-labeled TDP-43 was detected by high affinity HRP-conjugated streptavidin.

Detergent Solubility—Neuro2a cells were transiently transfected and differentiated by the above-mentioned method. Transfected cells were washed with PBS buffer three times and then collected by centrifugation at 1,000 × *g* for 5 min. Cells were lysed with 1% Triton X-100 (Sigma) in PBS buffer containing 1× complete protease inhibitor mixture (Roche Applied Science) and then incubated on ice for 10 min. This sample was separated by centrifugation at 20,000 × *g* for 10 min. The resultant supernatant was defined as the Triton X-100-soluble fraction. The pellet was solubilized by the same volume of 1% Sarkosyl (*N*-lauroylsarcosine, Sigma) in PBS buffer supplemented with 1× complete protease inhibitor mixture and then incubated on ice for 10 min. This sample was fractionated by centrifugation at 20,000 × *g* for 10 min. The resultant supernatant was defined as the Sarkosyl-soluble fraction, and then the final pellet was dissolved in 2% SDS in PBS buffer. The final pellet was defined as the Sarkosyl-insoluble fraction. The same volume of each fraction was separated by SDS-PAGE, and exogenous hTDP-43 was detected by an anti-human TDP-43 antibody. The immunoblotting results were quantified, and the percentage of TDP-43 contained in the Sarkosyl-insoluble fraction was calculated from the TDP-43 in all fractions.

Subcellular Fractionation—Neuro2a cells seeded in 6-well plates were transiently transfected by 0.5 μg of hTDP-43 expression vector and 1.25 μl of Lipofectamine^{TM} LTX (Invitrogen), followed by differentiation for 24 h. Transfected cells were sequentially solubilized by ProteoExtract^{TM} subcellular proteome kit (Merck). Cytoplasm, endoplasmic reticulum/mitochondria, and nuclear fractions were isolated by sequential solubilization and centrifugation according to the manufacturer's protocol. Exogenous hTDP-43 in each fraction was analyzed by SDS-PAGE. The ratio of nuclearly localized TDP-43 per total TDP-43 was calculated by the intensity of the bands detected by luminescent image analyzer (LAS-4000 Mini, Fujifilm, Japan).

TDP-43-stabilized Cell Models and Imaging—Neuro2a cells were transfected with a plasmid encoding a DD-fused TDP-43 (DD-TDP-43). Six hours after transfection, cells were differentiated with advanced DMEM/F12-GlutaMAX supplemented with 1% FBS and 2.5 mM Bt_2cAMP for 24 h, and 0.5 μM Shield1 was added for the indicated time until the cells were harvested for analysis. For imaging analysis, Neuro2a cells were cultured on Lab-Tek II-CC2-coated Chamber slides (Nunc), transfected with a DD-mCherry-hTDP-43 expression vector using Lipofectamine^{TM} 2000, differentiated, and stabilized with Shield1 as described above. The cells were fixed with 4% paraformaldehyde/phosphate buffer at the indicated time and stained with 2 μg/ml Hoechst 33342 (Invitrogen) for 15 min. The images were obtained by a confocal microscope (LSM5 Exciter, Carl Zeiss). To quantify the cells with DD-TDP-43 localized to the nucleus, more than 100 cells expressing DD-mCherry-TDP-43 per time point from three independent experiments were counted.

Cytotoxicity Analysis by FACS—Neuro2a cells seeded on 6-well plates were transfected with 2 μg of nontagged or DD-fused hTDP-43 expression vector using 5 μl of Lipofectamine^{TM} 2000. After 4 h of incubation, cells were differentiated with advanced DMEM/F12 (Invitrogen) supplemented with 100 units/ml penicillin G, GlutaMAX^{TM}, 1% FBS, and 2.5 mM Bt_2cAMP. Transfected cells were further incubated for 20 h

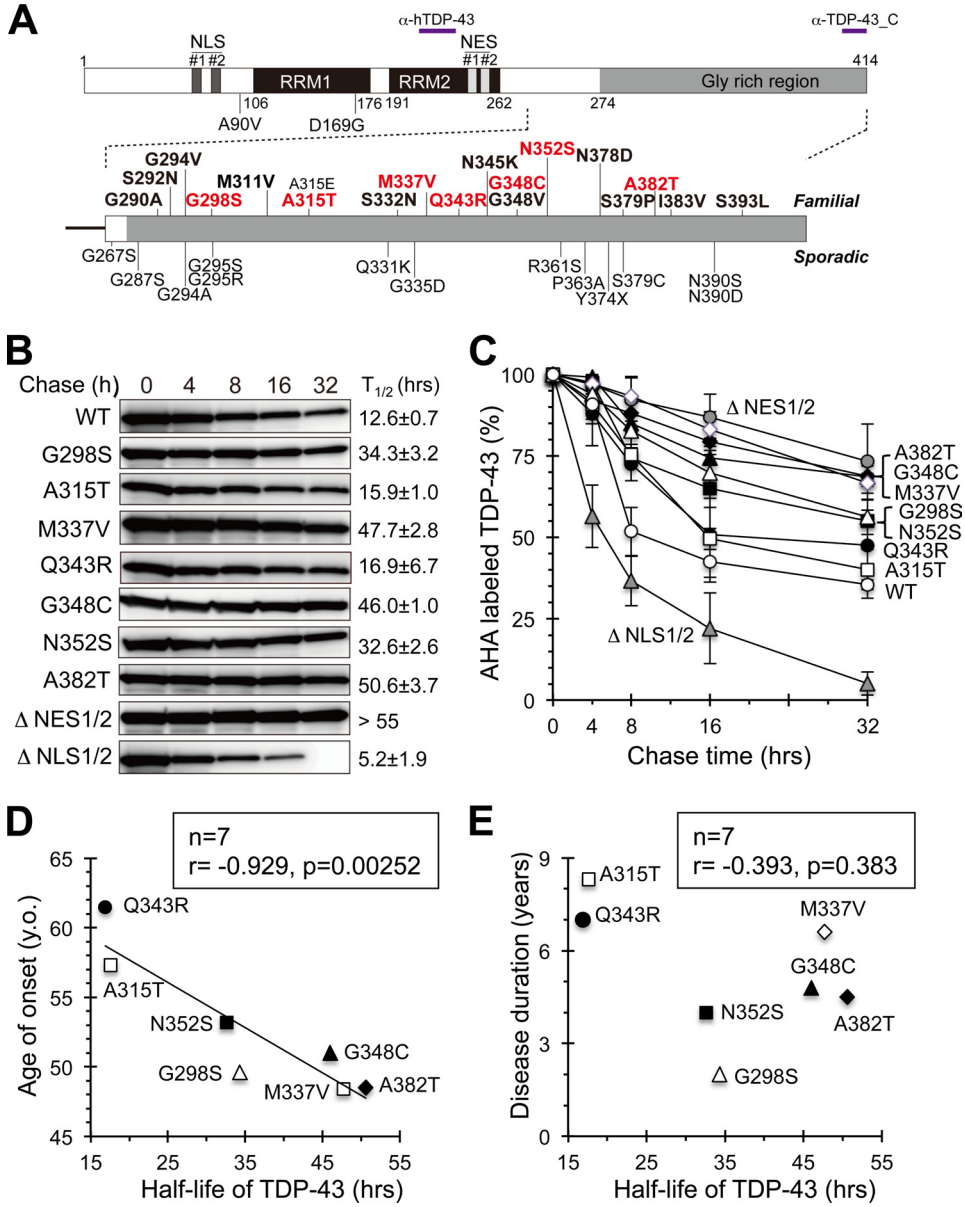

FIGURE 1. **Early disease onset correlates with increased stability of mutant TDP-43 proteins in familial ALS.** *A,* schematic drawing of human TDP-43 and its mutations. ALS-linked mutations of TDP-43 from familial (*upper*) and sporadic (*lower*) ALS cases as well as the locations of the NLS and NES are shown. The mutations used in our study are shown in *boldface type* (almost all familial ALS-linked mutations), and mutations with more than four patients are shown in *red*. The epitopes recognized by the anti-TDP-43 antibodies used in this study are indicated. *B* and *C,* half-lives of wild-type and mutant TDP-43 proteins. *B,* transfected Neuro2a cells were metabolically labeled with the methionine analog AHA. Labeled TDP-43 was immunoprecipitated and visualized by HRP-streptavidin as described under "Experimental Procedures." *C,* labeled TDP-43 bands were quantified, and the averages of three independent experiments were plotted. Half-lives of wild-type and mutant TDP-43 proteins were calculated by curve-fitting using this graph (*B, right*). *Error bars* represent S.E. *D* and *E,* half-lives of familial ALS-linked mutant TDP-43 proteins were negatively correlated with age of disease onset but not disease duration. Calculated half-lives of TDP-43 proteins were plotted against mean ages of disease onset (*D*) or duration (*E*). The correlations between each parameter and age of onset or duration were evaluated by the correlation coefficient (*r*) and probability (*p*) shown in each graph (*D* and *E*).

and treated with 0.5 μM Shield1 for the indicated times. After treatment with Shield1, cells were stained with 4.3 μM propidium iodide (PI). PI-positive cells were counted by FACS analysis (LSR-II, BD Biosciences).

Quantification of mRNA Levels by PCR—Total RNA was extracted from Neuro2a cells using TRIzol (Invitrogen) and RNeasy mini kit (Qiagen) according to manufacturer's instructions. cDNA was generated from 1 μg of total RNA using PrimeScript II first strand cDNA synthesis kit (Takara Bio, Japan), and 1/20th of the resulting cDNA was amplified with SYBR Premix Ex TaqII (Takara Bio) in a Thermal Cycler Dice Real Time System II (Takara Bio) under the following conditions: 1 cycle, 95 °C, 30 s; 50 cycles, 95 °C, 5 s and 60 °C, 30 s. Each sample was run in triplicate together with mouse *gapdh* control. Specific primers were mouse *TDP-43* forward, 5′-aatcagggtgggtttggtaaca-3′, and mouse *TDP-43* reverse, 5′-gctgggttaatgctaaaagcac-3′, which were adopted from PrimerBank at Massachusetts General Hospital (PrimerBank ID, 21704096a1), and mouse *GAPDH* forward, 5′-tgtgtccgtcgtggatctga-3′, and mouse *GAPDH* reverse, 5′-cctgcttcaccaccttcttga-3′.

TABLE 1

Clinical information of familial ALS patients with TDP-43 mutations

Clinical data were obtained from reports and confirmed by both Amyotrophic Lateral Sclerosis Online Genetics Database (ALSoD) and Alzheimer Disease and Frontotemporal Dementia Mutation Database (VIB Department of Molecular Genetics of the University of Antwerp, Belgium). Mean age of onset and duration for each mutation is listed with the references. Mutations with clinical information available from more than four patients are shown in boldface type. Detailed information for individual patients is provided in Table 2.

TDP-43 mutation	Mean onset (years old) (*n* of patients)[a]	Mean duration (years) (*n* of patients)[a]	No. of patients (*n* of family)	Ref.
G290A	49.0 (2)	1.0 (2)	2 (1)	42
S292N	61.0 (2)	3.0 (1)	2 (1)	43
G294V	71.5 (2)	2.0 (1)	3 (2)	44, 45
G298S	49.6 (**5**)	2.0 (**5**)	5 (1)	42, 46
M311V	44.0 (2)	2.8 (2)	4 (1)	47
A315T	57.3 (**6**)	8.0 (**4**)	6 (2)	48, 49
A315E	53.3 (3)	5.2 (2)	4 (1)	50
S332N	64.0 (1)	NA	1 (1)	44
M337V	48.4 (**17**)	6.6 (**11**)	17 (6)	44, 51–55
Q343R	61.5 (**4**)	7.0 (**2**)[b]	4 (1)	56
N345K	39.0 (1)	>4.0 (1)[c]	1 (1)	52
G348C	51.0 (**11**)	4.8 (**8**)	11 (2)	57, 58
G348V	54.5 (2)	2.4 (2)	3 (1)	51
N352S	53.2 (**4**)	4.0 (**2**)[b]	5 (2)	58, 59
N378D	46.0 (2)	2.1 (2)	2 (1)	55
S379P	40.0 (1)	NA	2 (1)	44
A382T	48.5 (**6**)	3.7 (**4**)	6 (4)	44, 49, 57
I383V	59.0 (1)	NA[d]	1 (1)	52
S393L	67.0 (1)	2.0 (1)	3 (1)	60

[a] The number of patients used to calculate mean onset or duration is shown.
[b] Two patients are still alive (Q343R; >3 or >1, N352S; >2 or >7 (years)).
[c] Single patient with this mutation is still alive.
[d] NA means the clinical information for disease duration not available.

Exon Skipping Assay—The exon skipping activity of hTDP-43 was determined by RT-PCR as described previously (19, 25). Neuro2a cells were co-transfected with 2.0 μg of pF5K-hTDP-43 DNA and 0.5 μg of pF5K-CFTR exon9 plasmids and differentiated for 24 h. Transfected cells were washed with PBS three times and then collected by centrifugation at 700 $\times$ *g* for 10 min. Total RNA was extracted from this cell pellet using an RNeasy mini kit (Qiagen). cDNA was synthesized by reverse transcription using 2.5 μg of total RNA and oligo(dT)$_{18}$ primer. CFTR exon9 fragments were amplified by cDNA and synthetic oligonucleotide pairs (α-2, 5′-caacttcaagctcctaagccactgc-3′, and Bra, 5′-taggatccggtcaccaggaagttggttaaatca-3′) in PCR, and PCR products were separated by 2% agarose gel. The exon skipping activity was calculated by the ratio of spliced PCR products per nonspliced ones.

Clinical Information and Statistics—Patient data from published articles describing TDP-43-linked familial ALS cases were summarized and confirmed with Amyotrophic Lateral Sclerosis Online Genetics Database and Alzheimer Disease and Frontotemporal Dementia Mutation Database (VIB Department of Molecular Genetics of the University of Antwerp, Belgium). Correlation of biochemical data with age of onset and disease duration was carried out by determination of Spearman rank correlation coefficient and significance.

RESULTS

Early Disease Onset Correlates with Stability of Mutant TDP-43 Proteins in Familial ALS—Protein mislocalization to cytoplasm, decreased detergent solubility, protein cleavage, and phosphorylation of TDP-43 are well documented characteristics of sporadic ALS lesions. To uncover the biochemical characteristics common among ALS-linked TDP-43 mutant proteins, we analyzed the degree of nuclear localization, detergent solubility, cleavage, phosphorylation, and stability of mutant TDP-43 proteins in a differentiated neuronal cell line.

First, we examined the half-lives of mutant TDP-43 proteins in differentiated neuronal cells with the use of the methionine analog L-azidohomoalanine to metabolically label newly synthesized proteins. Among 19 familial and 13 sporadic ALS-linked mutations (Fig. 1*A*), we chose to analyze seven familial ALS-linked TDP-43 mutations, for which detailed clinical information was available from a significant number of patients (more than four patients) (Fig. 1*A*, shown in *red*; Table 1, shown in boldface type). The half-lives of all mutant proteins ($t_{½}$ = 15.9–50.6 h) were consistently longer than that of wild-type protein ($t_{½}$ = 12.6 h) (Fig. 1, *B* and *C*). To examine whether stability of the mutant proteins correlates with patients' clinical course, we collected the available clinical information for ALS-linked familial TDP-43 mutations (Tables 1 and 2). Importantly, the patients carrying mutations with longer half-lives had earlier disease onset (p = 0.00252; Fig. 1*D*). No correlation, however, was observed between protein half-lives and duration of disease (Fig. 1*E*). Examination of the half-lives of localization mutants revealed that TDP-43 with mutations in the nuclear export signal (ΔNES1/2) exhibited an extremely long half-life ($t_{½}$ >55 h), whereas proteins with mutations in the nuclear localization signal (ΔNLS1/2) were less stable than wild-type protein ($t_{½}$ = 5.2 h) (Fig. 1, *B* and *C*).

Solubility and Localization of Mutant TDP-43 Are Not Correlated with Either Disease Onset or Duration—Because TDP-43 proteins in ALS lesions become insoluble to the detergent Sarkosyl, we analyzed the detergent solubility of wild-type and 18 familial ALS-linked mutant TDP-43 proteins by differential solubilization (Fig. 2*A*). Most mutant proteins exhibited lower Sarkosyl solubility than wild-type TDP-43 (Fig. 2, *B* and *C*). The subcellular localization of TDP-43 proteins was also analyzed (Fig. 3). The ratio of nuclear to total TDP-43 was measured in wild-type and mutant proteins, revealing that mutant TDP-43 demon-

TABLE 2

Detailed clinical information of familial ALS patients with TDP-43 mutations

Average (*n*) denotes mean onset or duration together with the number of patients with available clinical information. y.o. means years old.

TDP-43 mutation	Onset	Duration	Ref.
	years old	*years*	
G290A	47	1	42
	51	1	42
Average (*n*)	49 (2)	1.0 (2)	
S292N	58	3	43
	64	>3[a]	43
Average (*n*)	61 (2)	3.0 (1)	
G294V	77	NA[b]	44
	66	2	45
	NA	NA (65 y.o.)[c]	45
Average (*n*)	71.5 (2)	2.0 (1)	
G298S	47	1	42
	60	2	42
	48	1	42
	52	4	42
	41	2	42
	52	1.25	46
	45	2	46
	54	NA	46
Average (*n*)	49.8 (8)	1.9 (7)	
M311V	50	2.5	47
	38	3	47
	NA	NA (41 y.o.)[c]	47
	NA	NA (40 y.o.)[c]	47
Average (*n*)	44.0 (2)	2.8 (2)	
A315T	48	NA	48
	64	10	48
	72	7	48
	83	NA	48
	74	4	49
	47	11	49
Average (*n*)	57.3 (6)	8.0 (4)	
A315E	63	6	50
	57	4.33	50
	40	NA	50
	NA	NA (58 y.o.)	50
Average (*n*)	53.3 (3)	5.2 (2)	
S332N	64	NA	44
Average (*n*)	64.0 (1)	NA	
M337V	53	3	44
	47 (44–52: $n = 5$)[d]	5.5 ($n = 5$)[d]	53
	57	>4[a]	51
	42	17	51
	32	0.75	51
	55	6	51
	47	>5[a]	55
	57	>1[a]	55
	47	>11[a]	54
	55	>6[a]	54
	57	9	54
	48	10	54
	38	NA	52
Average (*n*)	48.4 (17)	6.6 (11)	
Q343R	57	>3[a]	56
	52	>1[a]	56
	75	2	56
	62	12	56
Average (*n*)	61.5 (4)	7.0 (2)	
N345K	39	>4[a]	52
Average (*n*)	39.0 (1)	>4.0[a]	
G348C	31	13	58
	55	3	58
	50	>3	57
	53	NA	57
	67	3–4	57
	39	3	57
	36	>3	57
	54	3	57
	66	4	57
	58	4	57
	53	5	57
Average (*n*)	51.0 (11)	4.8 (8)	
G348V	52	3	51
	57	1.75	51
	NA	NA (65 y.o.)[c]	51
Average (*n*)	54.5 (2)	2.4 (2)	
N352S	40	>7[a]	58
	50	4	58
	68	4	58
	NA	NA (42 y.o.)[c]	59
	55	>2[a]	59
Average (*n*)	53.2 (4)	4.0 (2)	
N378D	60	2.25	55
	32	2	55
Average (*n*)	46.0 (2)	2.1 (2)	
S379P	40	NA	44
	NA	NA (46 y.o.)[c]	44
Average (*n*)	40.0 (1)	NA	
A382T	32	3.5	44
	47	NA	44
	55	2.33	49
	57	6	49
	50	>5[a]	57
	50	3	57
Average (*n*)	48.5 (6)	3.7 (4)	
I383V	59	NA	52
Average (*n*)	59.0 (1)	NA	
S393L	67	2	60
	NA	NA (75 y.o.)[c]	60
	NA	NA	60
Average (*n*)	67.0 (1)	2.0 (1)	

[a] Number of patients are still alive. To calculate an average of disease duration, the data from live patients are excluded.
[b] NA indicates that the clinical information for disease onset or duration is not available.
[c] Age of death is available.
[d] Averaged onset or duration from five patients is available.

strated a slightly decreased tendency to localize to the nucleus than wild-type protein (Fig. 3*B*).

We then examined whether these biochemical properties correlated with the age of disease onset and disease duration of the patients carrying familial ALS-linked TDP-43 mutations (Table 1). We analyzed data from all mutations or from mutations affecting more than four patients, and neither relative tendency to Sarkosyl insolubility nor relative ratio of nucleus-localized TDP-43 was correlated with age of onset or duration of disease (Figs. 2*C* and 3*C*). Notably, ectopic expression of TDP-43 marginally induced cleavage of the protein, and no remarkable difference in the degree of phosphorylation was observed between wild-type and mutant TDP-43 proteins under our experimental conditions (data not shown).

Increased Stability of TDP-43 in Cells Leads to Protein Cleavage, Detergent Insolubility, and Cytotoxicity—Because increased stability of the proteins was observed consistently in ALS-linked TDP-43 mutants and protein stability was correlated with earlier disease onset, we next examined whether TDP-43 proteins with increased stability indicated altered biochemical and functional properties. To control the stability of TDP-43 proteins, we added a destabilizing domain of the FK-binding protein to the N terminus of TDP-43 (DD-TDP-43). DD-fused proteins become very unstable and are quickly degraded via the ubiquitin-proteasome pathway ($t_{1/2}$ = 15–30 min). However, when a membrane-permeable small compound called Shield1 is added, DD-fused proteins are stabilized (30) (Fig. 4*A*). When we stabilized DD-TDP-43 in the presence of Shield1, cleavage of TDP-43 protein and insolubility to the detergent Sarkosyl were markedly enhanced in a time-dependent manner (Fig. 4, *B–D*). The majority of cleaved TDP-43 product was detected in the Sarkosyl-insoluble fraction (Fig. 4,

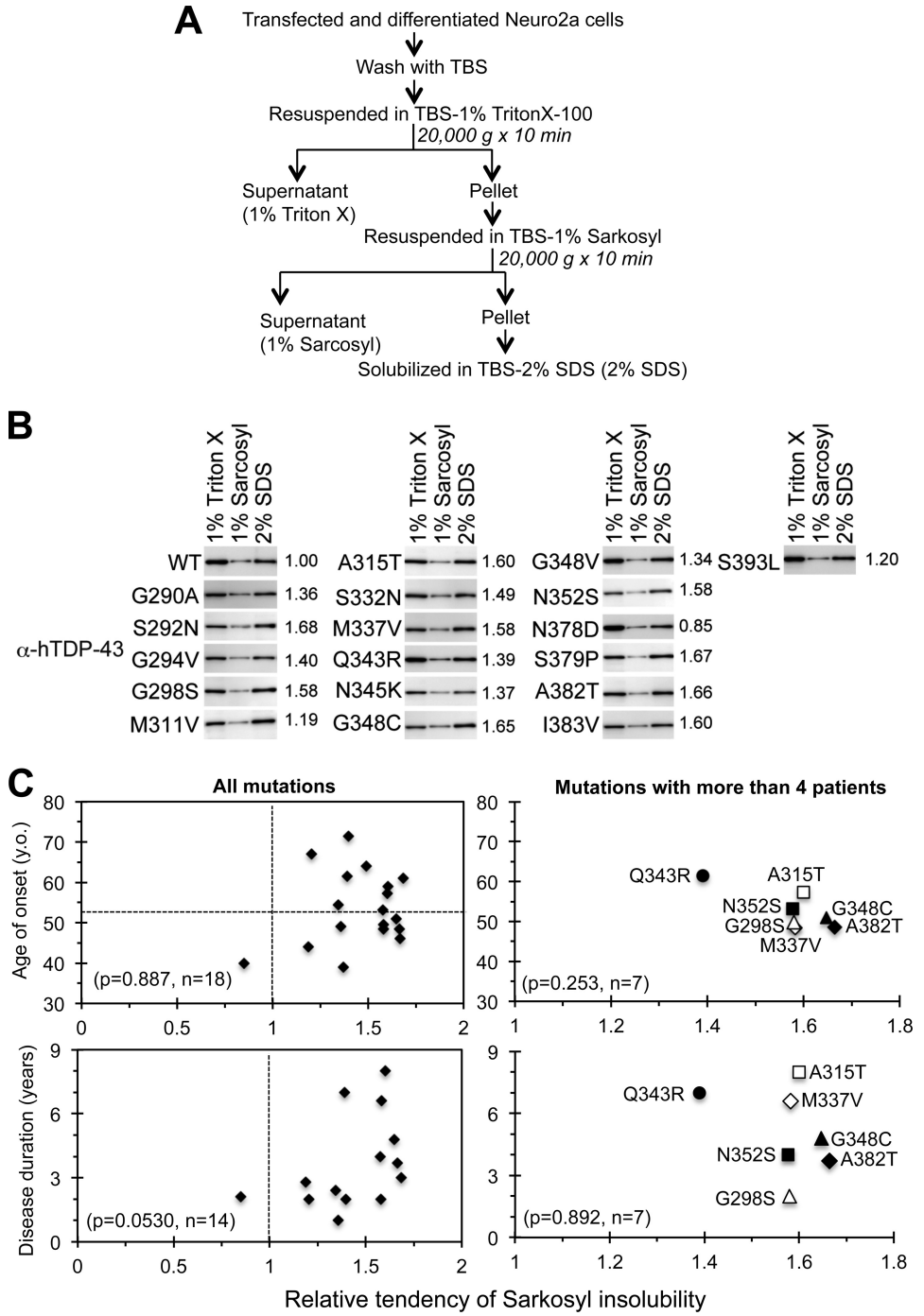

FIGURE 2. **Detergent insolubility of ALS-linked TDP-43 mutants is not correlated with onset or duration of disease.** *A* and *B,* determination of Sarkosyl solubility of exogenous human TDP-43 in differentiated Neuro2a cells. Neuro2a cells were transiently transfected with wild-type or ALS-linked mutant TDP-43 expression vectors and differentiated for 24 h. The solubility of human TDP-43 was determined by differential solubilization using three different detergents (Triton X-100, Sarkosyl, and SDS) as illustrated (*A*). Each fraction was analyzed by immunoblotting with anti-human TDP-43 antibody (*B*). *C,* solubility of ALS-linked TDP-43 mutants did not correlate with onset or duration of disease. The ratio of the amount of TDP-43 in the Sarkosyl-insoluble fraction (SDS-soluble fraction) to the total amount was normalized using the ratio of wild-type TDP-43 (*B, right*). Mean values from three independent experiments were used to calculate a relative tendency of Sarkosyl insolubility. Mean onset (*C, upper panels*) and duration (*C, lower panels*) of all familial ALS-linked mutations (*C, left panels*) or mutations in a significant number of patients (more than four) (*C, right panels*) were plotted against the relative ratios of Sarkosyl insolubility. The significance of correlation was evaluated by the probability (*p* value) shown in each graph. *y.o.*, years old.

C and *D*). Short term accumulation of DD-TDP-43 behaved similarly to the wild-type protein with respect to protein solubility and subcellular localization (Fig. 4, *E* and *F*), indicating that DD-TDP-43 acquires abnormal properties through a long term stabilization.

To test whether stabilized TDP-43 causes toxicity in the neuronal cells, we measured PI-positive cells in DD-TDP-43- or TDP-43-transfected cells in the presence of Shield1. Compared with TDP-43-transfected cells, accumulation of stabilized TDP-43 induced cytotoxicity in differentiated

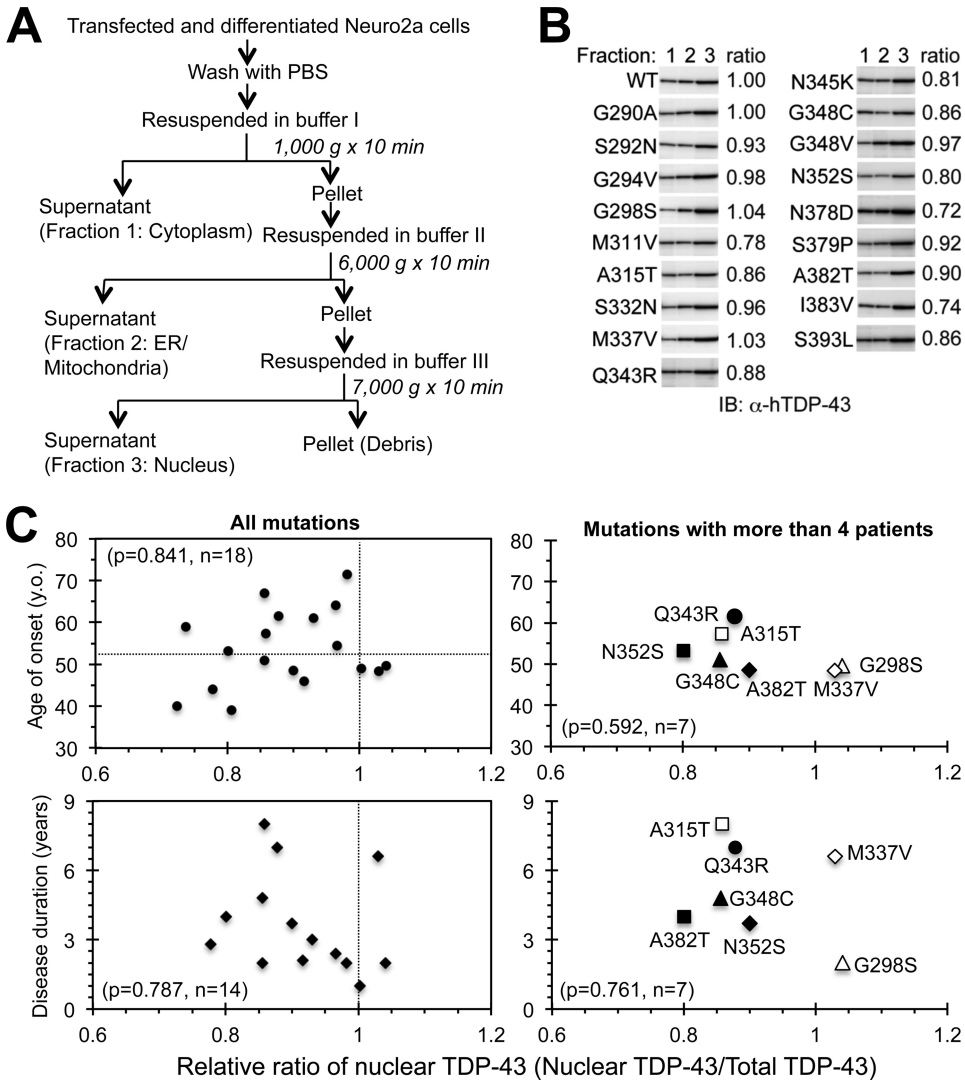

FIGURE 3. **Subcellular localization of TDP-43 is not correlated with disease onset or duration of mutant TDP-43-mediated ALS.** *A* and *B,* subcellular fractionation of differentiated Neuro2a cells expressed human TDP-43. Neuro2a cells were transiently transfected with wild-type or ALS-linked mutant TDP-43 expression vectors and differentiated with Bt_2cAMP. Cells were fractionated by differential centrifugation as illustrated (*A*). Subsequently, proteins in each fraction were analyzed by immunoblotting (*IB*) using anti-human TDP-43 antibody (*B*). *C,* subcellular localization of mutant TDP-43 proteins had no correlation with the time of disease onset or the disease duration. The ratio of nuclear fraction per total amount of TDP-43 protein in each mutant was calculated, normalized with the ratio of wild-type protein (*B*), and plotted with the mean onset age (*C, upper panel*) and the mean duration (*C, lower panel*) of each mutation. All familial ALS-linked TDP-43 mutations (*C, left panel*), or mutations with a significant number of patients (more than four) (*C, right panel*) were plotted. The significance of correlation was evaluated by the probability (*p* value) shown in each graph. *y.o.*, years old.

neuronal cells (Fig. 4, *G* and *H*). Finally, to examine the subcellular localization of stabilized TDP-43, we monitored the behavior of transfected DD-mCherry-TDP-43 protein (Fig. 5*A*). In the presence of Shield1, the expression level of stabilized DD-mCherry-TDP-43 protein was increased in a time-dependent manner (Fig. 5*B*). Most of the stabilized DD-mCherry-fused full-length TDP-43 was localized to the nucleus (Fig. 5, *B*–*H*), with nuclear aggregates in some cases (Fig. 5, *F* and *G*), suggesting that accumulation of stabilized TDP-43 in the nucleus was an important factor producing toxicity to neurons.

Dysregulation of TDP-43 mRNA Induced by Stabilized Wild-type TDP-43—Because TDP-43 has many roles in RNA metabolism, we examined whether TDP-43 stabilization affected the intrinsic functions of the protein in RNA regulation, such as autoregulation of *TDP-43* mRNA (9, 10). In differentiated neuronal cells, autoregulatory activity of wild-type TDP-43 was assessed by measuring the level of endogenous mouse *TDP-43* mRNA using quantitative reverse transcription-PCR (Fig. 6*A*). In the presence of exogenous hTDP-43 protein, levels of endogenous *TDP-43* mRNA were decreased in a dose-dependent manner (Fig. 6, *A*–*C*). However, stabilized TDP-43 caused dysregulation of *TDP-43* mRNA as compared with normal TDP-43 protein (0.1; *black bars*), with a similar protein level to DD-TDP-43 at 32 and 48 h (*white bars*; Fig. 6, *A* and *B*). By contrast, TDP-43 proteins with disease mutations retained their exon skipping activity on the CFTR mini-gene, which is another well characterized function of TDP-43 (8), performing comparably to wild-type TDP-43, which indicated that mutants did not lose this function (Fig. 7, *A*–*C*).

Stabilized TDP-43 Impairs Proteasome Activity—Determining whether accumulation of stabilized TDP-43 proteins affects

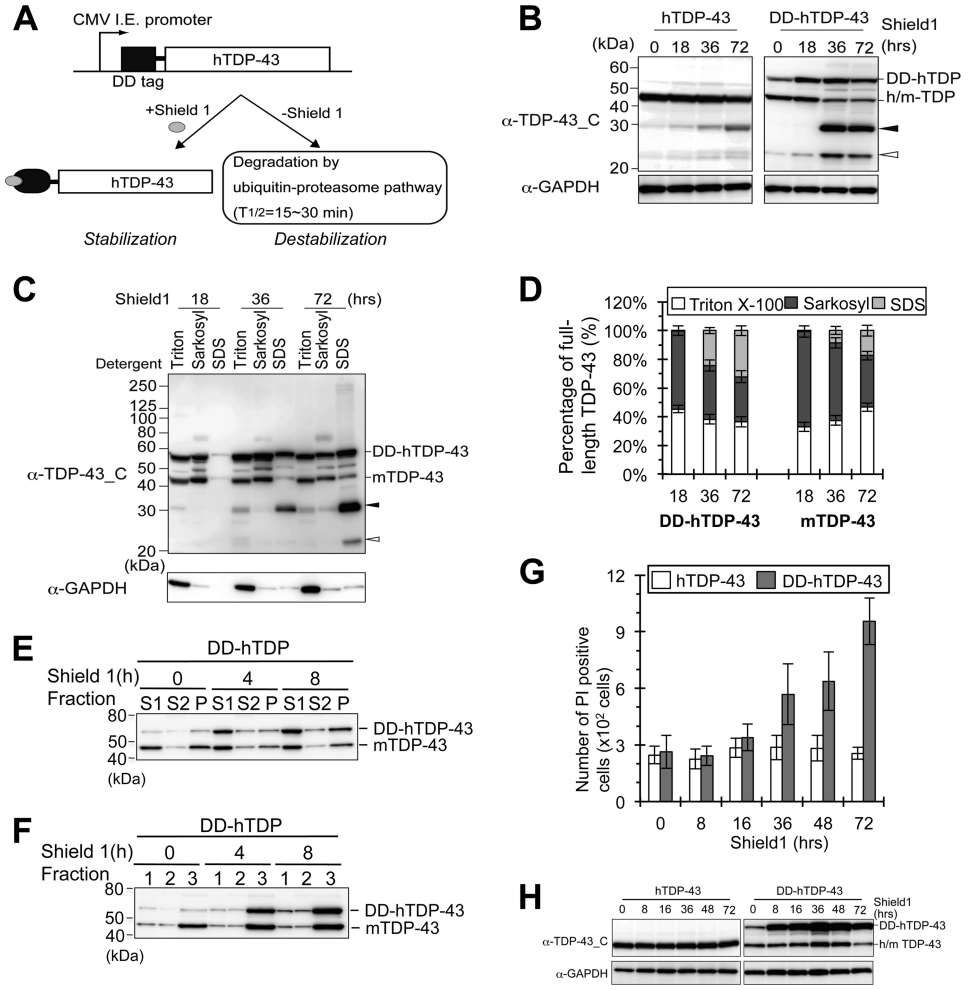

FIGURE 4. **Increased stability of TDP-43 leads to protein cleavage, detergent insolubility, and cytotoxicity in neuronal cells.** *A,* schematic diagram of the expression vector to control TDP-43 stability. *I.E.,* immediate early enhancer. *B,* cleavage of TDP-43 protein was increased by stabilized DD-fused TDP-43. Neuro2a cells were transfected with nontagged (hTDP-43) or DD-fused TDP-43 (DD-TDP-43), differentiated, and then incubated with Shield1 for the indicated time. Total protein extracts were analyzed by immunoblotting using antibodies directed against the TDP-43 C terminus (TDP-43_C) and GAPDH. Cleaved fragments of TDP-43 migrating to ~30 and 25 kDa are indicated with *black* and *white arrowheads*, respectively. *C* and *D,* detergent solubility of TDP-43 was decreased by stabilization of proteins. After stabilization for the indicated time, cells were sequentially solubilized by the indicated detergents. Each fraction was analyzed by immunoblotting using anti-TDP-43_C and GAPDH antibodies (*C*). *D,* percentage of full-length DD-TDP-43 or endogenous TDP-43 in each fraction measured in *C* was quantified. *E* and *F,* DD-hTDP-43 protein shares the similar properties with the endogenous wild-type TDP-43 during short term accumulation. Neuro2a cells were transiently transfected with DD-hTDP-43. DD-hTDP-43 was stabilized by incubation with Shield 1 for the indicated time. *E,* solubility of TDP-43 to the detergents was examined by the same method shown in Fig. 2. *S1,* 1% Triton X-100-soluble fraction; *S2,* 1% Sarkosyl-soluble fraction; *P,* 2% SDS-soluble fraction. *F,* subcellular localization of TDP-43 was analyzed by the same method shown in Fig. 3. Fraction 1, 2, and 3 indicate cytoplasm, endoplasmic reticulum/mitochondria, and nuclear fraction, respectively. *E* and *F,* each fraction was analyzed by immunoblotting using antibody against the TDP-43 C terminus (*TDP-43_C*). *G* and *H,* cytotoxicity was induced by stabilized TDP-43. Nontagged TDP-43 or DD-TDP-43 was transfected into Neuro2a cells. After incubation with Shield1 for the indicated time, cells were stained with PI. PI-positive cells were counted by FACS analysis (*G*). Expression levels of TDP-43 under the same conditions as *G* were confirmed by immunoblotting (*H*). Averages from three (*D*) or six (*G*) independent experiments are plotted, and *error bars* represent S.E.

proteostasis in neuronal cells is of great interest, because dysregulation of proteostasis is widely involved in the pathomechanisms of many neurodegenerative diseases. To monitor proteasome function, we constructed an expression vector encoding mutant ubiquitin-fused AcGFP (Fig. 8*A*). The ubiquitin-proteasome pathway rapidly degrades mutant Ub^{G76V}-fused proteins (27). When we stabilized TDP-43, proteasomal function as measured by accumulation of Ub^{G76V}-AcGFP was impaired in a time-dependent manner (Fig. 8, *B* and *C*). The proteasomal impairment was observed specifically in the presence of stabilized TDP-43 (Fig. 8*D*).

Finally, we monitored the fate of cleaved TDP-43 products, which prominently appeared in the presence of stabilized TDP-43. The levels of cleaved products migrating to ~30 and 25 kDa were substantially increased in the presence of the proteasome inhibitor MG132 or epoxomicin (Fig. 8*E*, *left panel*). By contrast, the amounts of those cleaved products were marginally affected when autophagy was inhibited or induced by the addition of wortmannin or rapamycin, respectively. When the lysosomal degradation pathway was inhibited in the presence of bafilomycin, the amount of 30-kDa cleaved product was slightly increased (Fig. 8*E*, *right panel*). Collectively, our results indicated that cleaved TDP-43 proteins were mainly degraded by the ubiquitin-proteasome pathway rather than an autophagy-lysosomal pathway, and the accumulation of cleaved proteins in the presence of stabilized TDP-43 was likely due to proteasomal impairment.

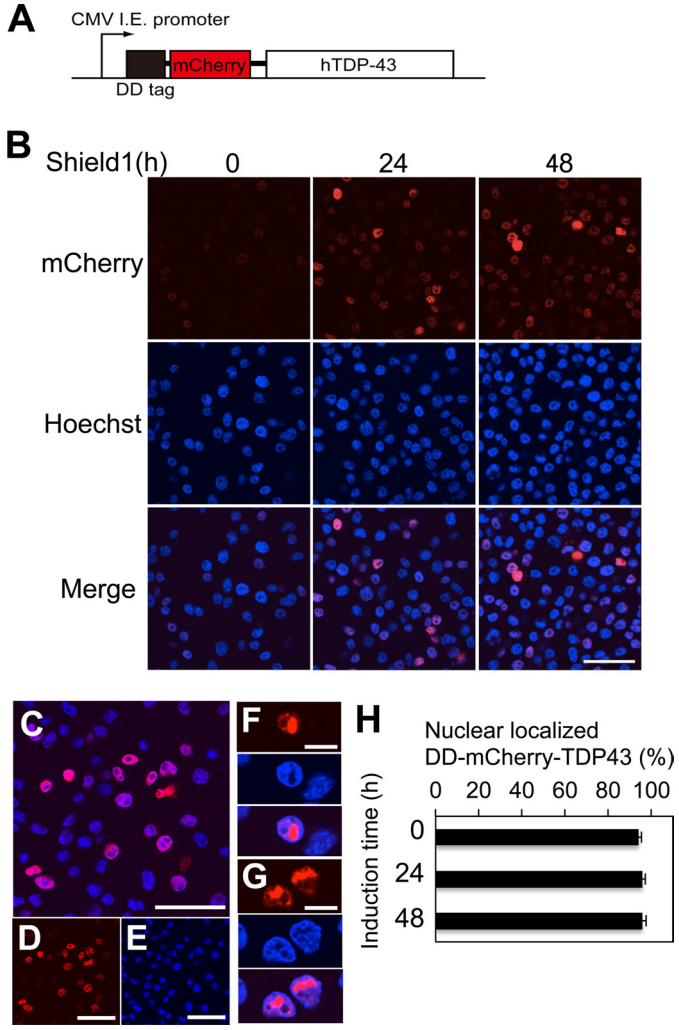

FIGURE 5. **Stabilized full-length TDP-43 proteins predominantly localize to the nucleus.** *A,* scheme for the plasmid encoding TDP-43 fused with both DD and mCherry (DD-mCherry-TDP-43) is illustrated. *B–H,* DD-mCherry-TDP-43 was stabilized by incubation with Shield1 for the indicated time in differentiated Neuro2a cells. DD-mCherry-TDP-43 was visualized by confocal microscopy. *I.E.,* immediate early enhancer. *B–G,* representative image of cells expressing stabilized DD-mCherry-TDP-43. *B,* representative confocal images of cells with stabilized TDP-43 for the indicated time visualized with mCherry, Hoechst, or both. *C–E,* confocal images of cells with stabilized TDP-43 for 24 h visualized with mCherry and Hoechst (*C*), mCherry (*D*), or Hoechst (*E*). *F* and *G,* cells with nuclear aggregates containing stabilized DD-mCherry-TDP-43 were visualized with mCherry (*top panel*), Hoechst (*middle panel*), or both (*bottom panel*). *H,* percentage of cells expressing nuclear TDP-43 among total mCherry-TDP-43 positive cells was calculated. Averages from three independent experiments are plotted. *Bars* represent S.E. *Bars B–E,* 50 μm; *F* and *G,* 10 μm.

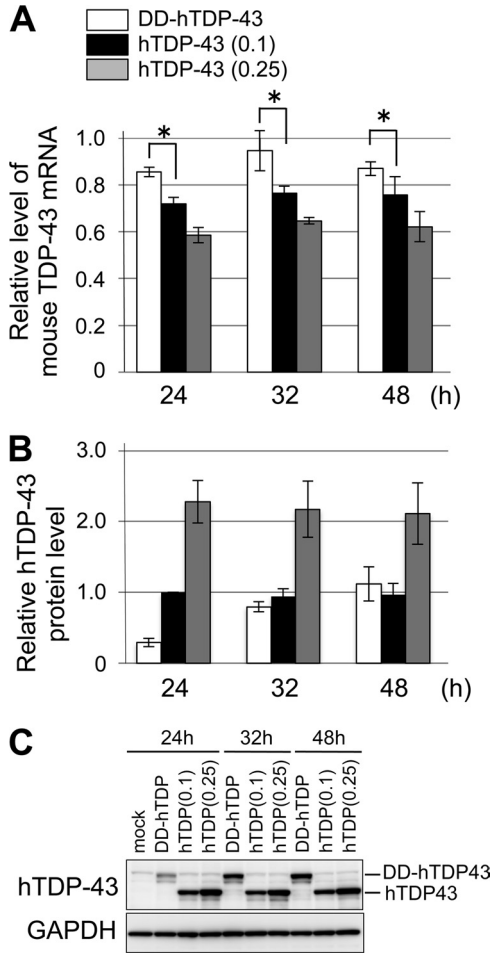

FIGURE 6. **Dysregulation of TDP-43 mRNA is caused by increased stability of wild-type TDP-43 protein.** *A,* reverse transcription-PCR analysis of endogenous mouse *TDP-43* mRNA in differentiated Neuro2a cells in the presence of DD-TDP-43 (*white bar*), hTDP-43 with transfection of 0.1 μg of plasmid (0.1; *black bar*), or hTDP-43 with transfection of 0.25 μg of plasmid (0.25; *gray bar*). *X* axis indicates the time after the initial transfection of the plasmids. *Y* axis denotes the levels of mouse *TDP-43* mRNA relative to those in mock-transfected cells. The mean value from four independent experiments was plotted.*, $p < 0.01$ (Student's *t* test). *B* and *C,* expression levels of exogenous DD-hTDP-43 and hTDP-43 proteins in the cells in *A* were measured by immunoblots using anti-hTDP-43 antibody (*C*). The quantification of DD-hTDP-43 and hTDP-43 proteins normalized to the levels of GAPDH was plotted (*B*).

DISCUSSION

Our attempt to identify the biochemical properties specific to disease-causing TDP-43 mutant proteins revealed that mutant TDP-43 proteins uniformly acquire longer half-lives than wild type. Importantly, ALS patients carrying mutant TDP-43 with a longer half-life show earlier disease onset, suggesting that increased stability of mutant TDP-43 could be a key phenomenon underlying mutant toxicities. Moreover, selective stabilization of wild-type TDP-43 in neuronal cells recapitulates biochemical characteristics of TDP-43 proteins in ALS tissue and elicits dysregulation of *TDP-43* mRNA, proteasomal impairment, and cytotoxicity, providing a novel cell model for TDP-43 proteinopathy.

The most striking finding in our study was that familial ALS patients carrying mutant TDP-43 with a longer half-life show earlier disease onset using seven representative familial TDP-43 mutations expressed in differentiated neuronal cells. This result is consistent with a previous study reporting that three TDP-43 mutants have longer half-lives in non-neuronal cells (22). To our knowledge, our study is the first report to describe a genotype-phenotype correlation in mutant TDP-43-carrying ALS patients based on the biochemical properties of mutant proteins, and it provides convincing evidence that the increased stability of mutant proteins plays a role in their toxicities and acceleration of disease onset. Several groups investigated the relationship between the biochemical characteristics of mutant proteins and the clinical course of human ALS patients with Cu,Zn-

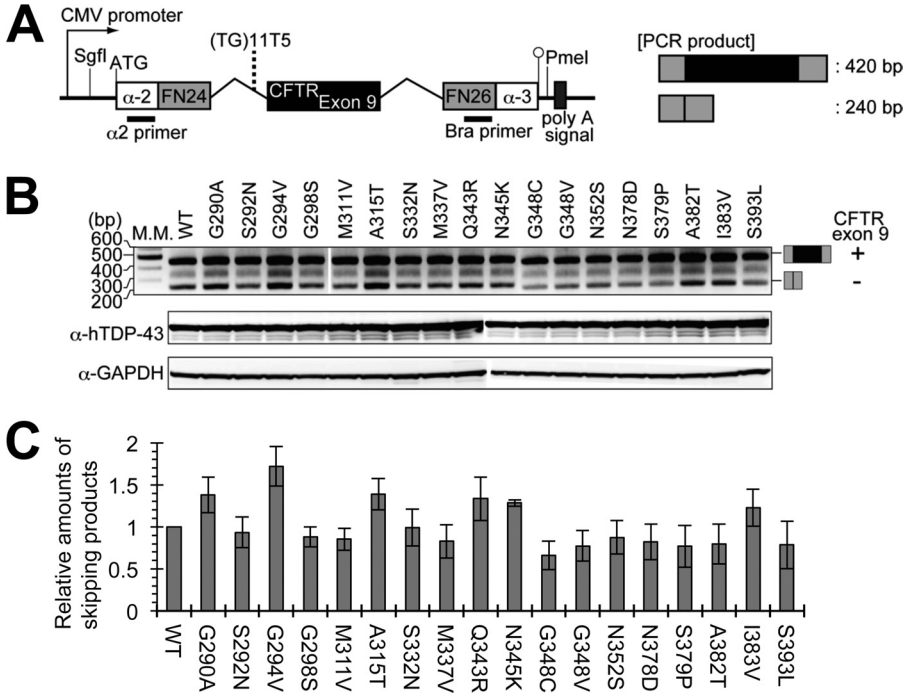

FIGURE 7. **Exon skipping activity is preserved in familial ALS-linked mutant TDP-43.** *A,* schematic drawing of CFTR mini-gene construct, which was developed with a modification of pTG11T5-hCFTR exon9, was illustrated (*A, left*). The size of PCR product after reverse transcription including (+) or excluding (−) exon9 is ~420 or 240 bp, respectively (*A, right*). *B,* Neuro2a cells were transiently co-transfected with both hTDP-43 and hCFTR mini-gene expression plasmids and then differentiated with Bt_2cAMP. Total RNAs were extracted from transfected cells, and cDNAs of hCFTR mini-gene including or excluding exon9 were amplified by the indicated primer pair (*a2, Bra*) after reverse transcription. The amplified PCR products were separated by electrophoresis using 1.5% agarose gel (*B, top*). To confirm expression levels of hTDP-43, total protein extracts were analyzed by immunoblotting using antibodies for human TDP-43 (*B, middle*) and GAPDH (*B, bottom*). *M.M.,* molecular marker. *C,* amounts of hCFTR PCR products, excluding exon9 in *B,* compared with wild-type TDP-43-transfected cells were plotted. Mean values from three independent experiments were plotted, and *error bars* represent S.E.

superoxide dismutase (SOD1) mutations, which are well known causes of inherited ALS. These studies elucidated that protein instability and higher aggregation propensity were determinants of disease progression (31–33). Although the number of patients carrying TDP-43 mutations is relatively small, our observation contrasts well with the cases of familial ALS with SOD1 mutations, because instability of mutant SOD1 correlates with accelerated disease progression, rather than age of disease onset (32). According to our previous finding that disease onset is determined by the toxicity within motor neurons in mutant SOD1 models (34), mutant TDP-43-mediated toxicity may be provoked mainly in motor neurons.

Several reports have demonstrated that overexpression of TDP-43 in cultured cells provokes toxicity to different degrees (20, 35). In these studies, protein cleavage and Sarkosyl insolubility were not clearly observed. By contrast, increased stability specific to DD-TDP-43 convincingly reproduced protein cleavage and decreased solubility to Sarkosyl, as well as dysregulation of *TDP-43* mRNA. In our stabilized TDP-43 cell models, 30- and 25-kDa C-terminal fragments were major components of the Sarkosyl-insoluble fraction as is consistent with our prior observation of the C terminus being a core of TDP-43 aggregates *in vitro* (36). Furthermore, stabilized TDP-43 impaired proteasomal function, with accumulation of 30- and 25-kDa cleaved fragments that were normally degraded by the proteasome. Our observation of stabilized TDP-43 impairs proteasome function rather than autophagy and is consistent with a recent report demonstrating that proteasome impairment, not an autophagy failure, leads to motor neuron degeneration in mice (37). Taken together, our results suggest that accumulation of misfolded C-terminal cleaved fragments of TDP-43 may disturb proteasome-mediated degradation, which may be one of the cytotoxic effects of misfolded TDP-43 species linked to the pathomechanisms of ALS and frontotemporal lobar degeneration.

Furthermore, our study suggests that a "dose effect" of TDP-43 plays a role in TDP-43-mediated neurodegeneration. Stabilized TDP-43 protein with a longer half-life may cause misregulation of its own mRNA, resulting in dysregulated translation of TDP-43 protein, which is misfolded, cleaved, and accumulated. Such a dose effect of TDP-43 protein is consistent with a recent observation of induced pluripotent stem cell-derived neurons from a TDP-43 mutation-carrying ALS patient expressing 2–4-fold higher levels of TDP-43 protein (38). Taken together, these results suggest that stabilized mutant TDP-43 with a longer half-life likely provokes a gain of toxicity leading to neurodegeneration. Because numerous RNA targets for TDP-43 have been identified through high throughput deep sequencing (10, 39, 40), TDP-43 mutants may also cause neurodegeneration through dysregulation of other mRNAs.

Finally, an important question remains regarding what subcellular compartment harbors the TDP-43 protein toxicity. Full-length TDP-43 protein carrying a mutation in the NLS was localized to the cytoplasm and had a shorter half-life than wild

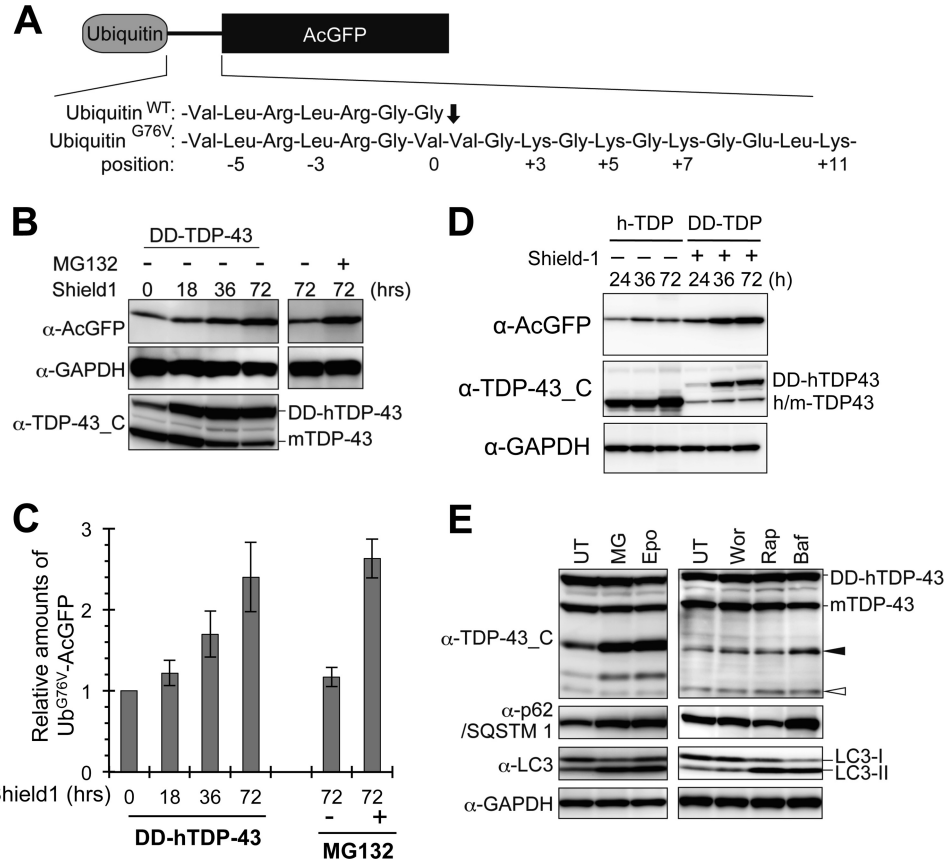

FIGURE 8. **Stabilized TDP-43 induces impairment of proteasome activity.** *A,* schematic drawing of the vector (Ub^{G76V}-AcGFP) for monitoring cellular proteasome activity. To facilitate proteasomal degradation of Ub^{G76V}-AcGFP in cells, four lysine residues were introduced to the linker sequence between mutant ubiquitin and AcGFP. *B* and *C,* proteasome activity was impaired by stabilized TDP-43. *B,* Neuro2a cells were co-transfected with DD-TDP-43 and Ub^{G76V}-AcGFP plasmids. DD-TDP-43 protein was stabilized using the same method shown in Fig. 3. Total cell extract was analyzed by immunoblotting using antibodies directed against AcGFP, TDP-43 C-terminal (*TDP-43_C*), and GAPDH. As a control experiment, Neuro2a cells were transfected with Ub^{G76V}-AcGFP in the absence or presence of 0.2 μM MG132 for 72 h (*right*). *C,* expression levels of Ub^{G76V}-AcGFP relative to that at 0 h are plotted. *D,* Neuro2a cells were co-transfected with Ub^{G76V}-AcGFP and hTDP-43 or DD-hTDP-43 using the same method shown in *B*. The levels of AcGFP, TDP-43, and GAPDH were analyzed by immunoblots. *E,* cleaved TDP-43 accumulated by proteasome inhibition, not autophagic inhibition. DD-TDP-43 was stabilized in Neuro2a cells, and the cells were then treated with the indicated reagents (*UT*, 0.1% DMSO; *MG*, 1 μM MG132; *Epo*, 0.25 μM epoxomicin; *Wor*, 0.1 μM wortmannin; *Rap*, 0.5 μM rapamycin; *Baf*, 0.1 μM bafilomycin A1) for 16 h. After treatment, total protein extracts were analyzed by immunoblotting using antibodies directed against TDP-43_C, p62/SQSTM1, LC3, and GAPDH (*E*). TDP-43 fragments of 30 and 25 kDa are indicated with *black* and *white arrowheads*, respectively.

type (Fig. 1, *B* and *C*). The C-terminal fragment of TDP-43 has also been characterized as unstable in cultured cells (41). By contrast, TDP-43 with an NES-deficient mutation, in which protein export from the nucleus is disturbed, has an extremely long half-life, similar to the proteins harboring disease-causing mutations (Fig. 1, *B* and *C*). We speculate that the disease-causing mutants with longer half-lives initially produce unidentified toxicity in the nucleus, perhaps including dysregulation of mRNAs, which chronically elevates expression levels of TDP-43 protein to ultimately result in protein misfolding, cleavage, and aggregation.

In summary, we discovered that accelerated disease onset in the familial ALS patients is correlated with TDP-43 mutations that increase protein half-life. We also established a new cell model to control the stability of TDP-43 that offers insight into the disease mechanism and significance of protein stability. Increased stability of TDP-43 provokes protein misfolding, leading to insolubility to detergents, protein cleavage, proteasomal impairment, and cytotoxicity. Identifying mechanisms through which ALS-linked mutant TDP-43 is stabilized, including abnormal protein interactions with other ALS-linked proteins, such as fused in sarcoma (22), or as-yet unidentified proteins, will be crucial to uncovering the pathological triggers of neurodegeneration in ALS.

Acknowledgments—We thank the members of Yamanaka Laboratory and Dr. Yoshiaki Furukawa for valuable discussions and suggestions, Dr. Francisco Baralle for the pTG11T5-hCFTR exon9 construct, and the Support Unit for Bio-material Analysis in RIKEN BSI Research Resources Center for supporting FACS and DNA analysis.

REFERENCES

1. Neumann, M., Sampathu, D. M., Kwong, L. K., Truax, A. C., Micsenyi, M. C., Chou, T. T., Bruce, J., Schuck, T., Grossman, M., Clark, C. M., McCluskey, L. F., Miller, B. L., Masliah, E., Mackenzie, I. R., Feldman, H., Feiden, W., Kretzschmar, H. A., Trojanowski, J. Q., and Lee, V. M. (2006) Ubiquitinated TDP-43 in frontotemporal lobar degeneration and amyotrophic lateral sclerosis. *Science* **314,** 130–133
2. Arai, T., Hasegawa, M., Akiyama, H., Ikeda, K., Nonaka, T., Mori, H., Mann, D., Tsuchiya, K., Yoshida, M., Hashizume, Y., and Oda, T. (2006) TDP-43 is a component of ubiquitin-positive tau-negative inclusions in

frontotemporal lobar degeneration and amyotrophic lateral sclerosis. *Biochem. Biophys. Res. Commun.* **351,** 602–611
3. Chen-Plotkin, A. S., Lee, V. M., and Trojanowski, J. Q. (2010) TAR DNA-binding protein 43 in neurodegenerative disease. *Nat. Rev. Neurol.* **6,** 211–220
4. Cohen, T. J., Lee, V. M., and Trojanowski, J. Q. (2011) TDP-43 functions and pathogenic mechanisms implicated in TDP-43 proteinopathies. *Trends Mol. Med.* **17,** 659–667
5. Lagier-Tourenne, C., and Cleveland, D. W. (2009) Rethinking ALS. The FUS about TDP-43. *Cell* **136,** 1001–1004
6. Pesiridis, G. S., Lee, V. M., and Trojanowski, J. Q. (2009) Mutations in TDP-43 link glycine-rich domain functions to amyotrophic lateral sclerosis. *Hum. Mol. Genet.* **18,** R156–R162
7. Lagier-Tourenne, C., Polymenidou, M., and Cleveland, D. W. (2010) TDP-43 and FUS/TLS. Emerging roles in RNA processing and neurodegeneration. *Hum. Mol. Genet.* **19,** R46–R64
8. Buratti, E., and Baralle, F. E. (2010) The multiple roles of TDP-43 in pre-mRNA processing and gene expression regulation. *RNA Biol.* **7,** 420–429
9. Ayala, Y. M., De Conti, L., Avendaño-Vázquez, S. E., Dhir, A., Romano, M., D'Ambrogio, A., Tollervey, J., Ule, J., Baralle, M., Buratti, E., and Baralle, F. E. (2011) TDP-43 regulates its mRNA levels through a negative feedback loop. *EMBO J.* **30,** 277–288
10. Polymenidou, M., Lagier-Tourenne, C., Hutt, K. R., Huelga, S. C., Moran, J., Liang, T. Y., Ling, S. C., Sun, E., Wancewicz, E., Mazur, C., Kordasiewicz, H., Sedaghat, Y., Donohue, J. P., Shiue, L., Bennett, C. F., Yeo, G. W., and Cleveland, D. W. (2011) Long pre-mRNA depletion and RNA missplicing contribute to neuronal vulnerability from loss of TDP-43. *Nat. Neurosci.* **14,** 459–468
11. Wils, H., Kleinberger, G., Janssens, J., Pereson, S., Joris, G., Cuijt, I., Smits, V., Ceuterick-de Groote, C., Van Broeckhoven, C., and Kumar-Singh, S. (2010) TDP-43 transgenic mice develop spastic paralysis and neuronal inclusions characteristic of ALS and frontotemporal lobar degeneration. *Proc. Natl. Acad. Sci. U.S.A.* **107,** 3858–3863
12. Shan, X., Chiang, P. M., Price, D. L., and Wong, P. C. (2010) Altered distributions of Gemini of coiled bodies and mitochondria in motor neurons of TDP-43 transgenic mice. *Proc. Natl. Acad. Sci. U.S.A.* **107,** 16325–16330
13. Xu, Y. F., Gendron, T. F., Zhang, Y. J., Lin, W. L., D'Alton, S., Sheng, H., Casey, M. C., Tong, J., Knight, J., Yu, X., Rademakers, R., Boylan, K., Hutton, M., McGowan, E., Dickson, D. W., Lewis, J., and Petrucelli, L. (2010) Wild-type human TDP-43 expression causes TDP-43 phosphorylation, mitochondrial aggregation, motor deficits, and early mortality in transgenic mice. *J. Neurosci.* **30,** 10851–10859
14. Tsai, K. J., Yang, C. H., Fang, Y. H., Cho, K. H., Chien, W. L., Wang, W. T., Wu, T. W., Lin, C. P., Fu, W. M., and Shen, C. K. (2010) Elevated expression of TDP-43 in the forebrain of mice is sufficient to cause neurological and pathological phenotypes mimicking FTLD-U. *J. Exp. Med.* **207,** 1661–1673
15. Sephton, C. F., Good, S. K., Atkin, S., Dewey, C. M., Mayer, P., 3rd, Herz, J., and Yu, G. (2010) TDP-43 is a developmentally regulated protein essential for early embryonic development. *J. Biol. Chem.* **285,** 6826–6834
16. Wu, L. S., Cheng, W. C., Hou, S. C., Yan, Y. T., Jiang, S. T., and Shen, C. K. (2010) TDP-43, a neuro-pathosignature factor, is essential for early mouse embryogenesis. *Genesis* **48,** 56–62
17. Kraemer, B. C., Schuck, T., Wheeler, J. M., Robinson, L. C., Trojanowski, J. Q., Lee, V. M., and Schellenberg, G. D. (2010) Loss of murine TDP-43 disrupts motor function and plays an essential role in embryogenesis. *Acta Neuropathol.* **119,** 409–419
18. Johnson, B. S., McCaffery, J. M., Lindquist, S., and Gitler, A. D. (2008) A yeast TDP-43 proteinopathy model. Exploring the molecular determinants of TDP-43 aggregation and cellular toxicity. *Proc. Natl. Acad. Sci. U.S.A.* **105,** 6439–6444
19. Nonaka, T., Kametani, F., Arai, T., Akiyama, H., and Hasegawa, M. (2009) Truncation and pathogenic mutations facilitate the formation of intracellular aggregates of TDP-43. *Hum. Mol. Genet.* **18,** 3353–3364
20. Guo, W., Chen, Y., Zhou, X., Kar, A., Ray, P., Chen, X., Rao, E. J., Yang, M., Ye, H., Zhu, L., Liu, J., Xu, M., Yang, Y., Wang, C., Zhang, D., Bigio, E. H., Mesulam, M., Shen, Y., Xu, Q., Fushimi, K., and Wu, J. Y. (2011) An ALS-associated mutation affecting TDP-43 enhances protein aggregation, fibril formation, and neurotoxicity. *Nat. Struct. Mol. Biol.* **18,** 822–830
21. Barmada, S. J., Skibinski, G., Korb, E., Rao, E. J., Wu, J. Y., and Finkbeiner, S. (2010) Cytoplasmic mislocalization of TDP-43 is toxic to neurons and enhanced by a mutation associated with familial amyotrophic lateral sclerosis. *J. Neurosci.* **30,** 639–649
22. Ling, S. C., Albuquerque, C. P., Han, J. S., Lagier-Tourenne, C., Tokunaga, S., Zhou, H., and Cleveland, D. W. (2010) ALS-associated mutations in TDP-43 increase its stability and promote TDP-43 complexes with FUS/TLS. *Proc. Natl. Acad. Sci. U.S.A.* **107,** 13318–13323
23. Da Cruz, S., and Cleveland, D. W. (2011) Understanding the role of TDP-43 and FUS/TLS in ALS and beyond. *Curr. Opin. Neurobiol.* **21,** 904–919
24. Winton, M. J., Igaz, L. M., Wong, M. M., Kwong, L. K., Trojanowski, J. Q., and Lee, V. M. (2008) Disturbance of nuclear and cytoplasmic TAR DNA-binding protein (TDP-43) induces disease-like redistribution, sequestration, and aggregate formation. *J. Biol. Chem.* **283,** 13302–13309
25. Pagani, F., Buratti, E., Stuani, C., Romano, M., Zuccato, E., Niksic, M., Giglio, L., Faraguna, D., and Baralle, F. E. (2000) Splicing factors induce cystic fibrosis transmembrane regulator exon9 skipping through a nonevolutionary conserved intronic element. *J. Biol. Chem.* **275,** 21041–21047
26. D'Ambrogio, A., Buratti, E., Stuani, C., Guarnaccia, C., Romano, M., Ayala, Y. M., and Baralle, F. E. (2009) Functional mapping of the interaction between TDP-43 and hnRNP A2 *in vivo*. *Nucleic Acids Res.* **37,** 4116–4126
27. Dantuma, N. P., Lindsten, K., Glas, R., Jellne, M., and Masucci, M. G. (2000) Short-lived green fluorescent proteins for quantifying ubiquitin/proteasome-dependent proteolysis in living cells. *Nat. Biotechnol.* **18,** 538–543
28. Tremblay, R. G., Sikorska, M., Sandhu, J. K., Lanthier, P., Ribecco-Lutkiewicz, M., and Bani-Yaghoub, M. (2010) Differentiation of mouse Neuro 2A cells into dopamine neurons. *J. Neurosci. Methods* **186,** 60–67
29. Matsuyama, S., Fujita, Y., and Mizushima, S. (1993) SecD is involved in the release of translocated secretory proteins from the cytoplasmic membrane of *Escherichia coli*. *EMBO J.* **12,** 265–270
30. Banaszynski, L. A., Chen, L. C., Maynard-Smith, L. A., Ooi, A. G., and Wandless, T. J. (2006) A rapid, reversible, and tunable method to regulate protein function in living cells using synthetic small molecules. *Cell* **126,** 995–1004
31. Prudencio, M., Hart, P. J., Borchelt, D. R., and Andersen, P. M. (2009) Variation in aggregation propensities among ALS-associated variants of SOD1. Correlation to human disease. *Hum. Mol. Genet.* **18,** 3217–3226
32. Sato, T., Nakanishi, T., Yamamoto, Y., Andersen, P. M., Ogawa, Y., Fukada, K., Zhou, Z., Aoike, F., Sugai, F., Nagano, S., Hirata, S., Ogawa, M., Nakano, R., Ohi, T., Kato, T., Nakagawa, M., Hamasaki, T., Shimizu, A., and Sakoda, S. (2005) Rapid disease progression correlates with instability of mutant SOD1 in familial ALS. *Neurology* **65,** 1954–1957
33. Wang, Q., Johnson, J. L., Agar, N. Y., and Agar, J. N. (2008) Protein aggregation and protein instability govern familial amyotrophic lateral sclerosis patient survival. *PLoS Biol.* **6,** e170
34. Boillée, S., Yamanaka, K., Lobsiger, C. S., Copeland, N. G., Jenkins, N. A., Kassiotis, G., Kollias, G., and Cleveland, D. W. (2006) Onset and progression in inherited ALS determined by motor neurons and microglia. *Science* **312,** 1389–1392
35. Kabashi, E., Lin, L., Tradewell, M. L., Dion, P. A., Bercier, V., Bourgouin, P., Rochefort, D., Bel Hadj, S., Durham, H. D., Vande Velde, C., Rouleau, G. A., and Drapeau, P. (2010) Gain and loss of function of ALS-related mutations of TARDBP (TDP-43) cause motor deficits *in vivo*. *Hum. Mol. Genet.* **19,** 671–683
36. Furukawa, Y., Kaneko, K., Watanabe, S., Yamanaka, K., and Nukina, N. (2011) A seeding reaction recapitulates intracellular formation of Sarkosyl-insoluble transactivation response element (TAR) DNA-binding protein-43 inclusions. *J. Biol. Chem.* **286,** 18664–18672
37. Tashiro, Y., Urushitani, M., Inoue, H., Koike, M., Uchiyama, Y., Komatsu, M., Tanaka, K., Yamazaki, M., Abe, M., Misawa, H., Sakimura, K., Ito, H., and Takahashi, R. (2012) Motor neuron-specific disruption of proteasomes, but not autophagy, replicates amyotrophic lateral sclerosis. *J. Biol.*

Chem. **287,** 42984–42994
38. Bilican, B., Serio, A., Barmada, S. J., Nishimura, A. L., Sullivan, G. J., Carrasco, M., Phatnani, H. P., Puddifoot, C. A., Story, D., Fletcher, J., Park, I. H., Friedman, B. A., Daley, G. Q., Wyllie, D. J., Hardingham, G. E., Wilmut, I., Finkbeiner, S., Maniatis, T., Shaw, C. E., and Chandran, S. (2012) Mutant induced pluripotent stem cell lines recapitulate aspects of TDP-43 proteinopathies and reveal cell-specific vulnerability. *Proc. Natl. Acad. Sci. U.S.A.* **109,** 5803–5808
39. Sephton, C. F., Cenik, C., Kucukural, A., Dammer, E. B., Cenik, B., Han, Y., Dewey, C. M., Roth, F. P., Herz, J., Peng, J., Moore, M. J., and Yu, G. (2011) Identification of neuronal RNA targets of TDP-43-containing ribonucleoprotein complexes. *J. Biol. Chem.* **286,** 1204–1215
40. Tollervey, J. R., Curk, T., Rogelj, B., Briese, M., Cereda, M., Kayikci, M., König, J., Hortobágyi, T., Nishimura, A. L., Zupunski, V., Patani, R., Chandran, S., Rot, G., Zupan, B., Shaw, C. E., and Ule, J. (2011) Characterizing the RNA targets and position-dependent splicing regulation by TDP-43. *Nat. Neurosci.* **14,** 452–458
41. Pesiridis, G. S., Tripathy, K., Tanik, S., Trojanowski, J. Q., and Lee, V. M. (2011) A "two-hit" hypothesis for inclusion formation by carboxyl-terminal fragments of TDP-43 protein linked to RNA depletion and impaired microtubule-dependent transport. *J. Biol. Chem.* **286,** 18845–18855
42. Van Deerlin, V. M., Leverenz, J. B., Bekris, L. M., Bird, T. D., Yuan, W., Elman, L. B., Clay, D., Wood, E. M., Chen-Plotkin, A. S., Martinez-Lage, M., Steinbart, E., McCluskey, L., Grossman, M., Neumann, M., Wu, I. L., Yang, W. S., Kalb, R., Galasko, D. R., Montine, T. J., Trojanowski, J. Q., Lee, V. M., Schellenberg, G. D., and Yu, C. E. (2008) TARDBP mutations in amyotrophic lateral sclerosis with TDP-43 neuropathology. A genetic and histopathological analysis. *Lancet Neurol.* **7,** 409–416
43. Xiong, H. L., Wang, J. Y., Sun, Y. M., Wu, J. J., Chen, Y., Qiao, K., Zheng, Q. J., Zhao, G. X., and Wu, Z. Y. (2010) Association between novel TARDBP mutations and Chinese patients with amyotrophic lateral sclerosis. *BMC Med. Genet.* **11,** 8
44. Corrado, L., Ratti, A., Gellera, C., Buratti, E., Castellotti, B., Carlomagno, Y., Ticozzi, N., Mazzini, L., Testa, L., Taroni, F., Baralle, F. E., Silani, V., and D'Alfonso, S. (2009) High frequency of TARDBP gene mutations in Italian patients with amyotrophic lateral sclerosis. *Hum. Mutat.* **30,** 688–694
45. Williams, K. L., Durnall, J. C., Thoeng, A. D., Warraich, S. T., Nicholson, G. A., and Blair, I. P. (2009) A novel TARDBP mutation in an Australian amyotrophic lateral sclerosis kindred. *J. Neurol. Neurosurg. Psychiatry* **80,** 1286–1288
46. Nozaki, I., Arai, M., Takahashi, K., Hamaguchi, T., Yoshikawa, H., Muroishi, T., Noguchi-Shinohara, M., Ito, H., Itokawa, M., Akiyama, H., Kawata, A., and Yamada, M. (2010) Familial ALS with G298S mutation in TARDBP: a comparison of CSF Tau protein levels with those in sporadic ALS. *Intern. Med.* **49,** 1209–1212
47. Lemmens, R., Race, V., Hersmus, N., Matthijs, G., Van Den Bosch, L., Van Damme, P., Dubois, B., Boonen, S., Goris, A., and Robberecht, W. (2009) TDP-43 M311V mutation in familial amyotrophic lateral sclerosis. *J. Neurol. Neurosurg. Psychiatry* **80,** 354–355
48. Gitcho, M. A., Baloh, R. H., Chakraverty, S., Mayo, K., Norton, J. B., Levitch, D., Hatanpaa, K. J., White, C. L., 3rd, Bigio, E. H., Caselli, R., Baker, M., Al-Lozi, M. T., Morris, J. C., Pestronk, A., Rademakers, R., Goate, A. M., and Cairns, N. J. (2008) TDP-43 A315T mutation in familial motor neuron disease. *Ann. Neurol.* **63,** 535–538
49. Kabashi, E., Valdmanis, P. N., Dion, P., Spiegelman, D., McConkey, B. J., Vande Velde, C., Bouchard, J. P., Lacomblez, L., Pochigaeva, K., Salachas, F., Pradat, P. F., Camu, W., Meininger, V., Dupre, N., and Rouleau, G. A. (2008) TARDBP mutations in individuals with sporadic and familial amyotrophic lateral sclerosis. *Nat. Genet.* **40,** 572–574
50. Fujita, Y., Ikeda, M., Yanagisawa, T., Senoo, Y., and Okamoto, K. (2011) Different clinical and neuropathologic phenotypes of familial ALS with A315E TARDBP mutation. *Neurology* **77,** 1427–1431
51. Kirby, J., Goodall, E. F., Smith, W., Highley, J. R., Masanzu, R., Hartley, J. A., Hibberd, R., Hollinger, H. C., Wharton, S. B., Morrison, K. E., Ince, P. G., McDermott, C. J., and Shaw, P. J. (2010) Broad clinical phenotypes associated with TAR-DNA-binding protein (TARDBP) mutations in amyotrophic lateral sclerosis. *Neurogenetics* **11,** 217–225
52. Rutherford, N. J., Zhang, Y. J., Baker, M., Gass, J. M., Finch, N. A., Xu, Y. F., Stewart, H., Kelley, B. J., Kuntz, K., Crook, R. J., Sreedharan, J., Vance, C., Sorenson, E., Lippa, C., Bigio, E. H., Geschwind, D. H., Knopman, D. S., Mitsumoto, H., Petersen, R. C., Cashman, N. R., Hutton, M., Shaw, C. E., Boylan, K. B., Boeve, B., Graff-Radford, N. R., Wszolek, Z. K., Caselli, R. J., Dickson, D. W., Mackenzie, I. R., Petrucelli, L., and Rademakers, R. (2008) Novel mutations in TARDBP (TDP-43) in patients with familial amyotrophic lateral sclerosis. *PLoS Genet.* **4,** e1000193
53. Sreedharan, J., Blair, I. P., Tripathi, V. B., Hu, X., Vance, C., Rogelj, B., Ackerley, S., Durnall, J. C., Williams, K. L., Buratti, E., Baralle, F., de Belleroche, J., Mitchell, J. D., Leigh, P. N., Al-Chalabi, A., Miller, C. C., Nicholson, G., and Shaw, C. E. (2008) TDP-43 mutations in familial and sporadic amyotrophic lateral sclerosis. *Science* **319,** 1668–1672
54. Tamaoka, A., Arai, M., Itokawa, M., Arai, T., Hasegawa, M., Tsuchiya, K., Takuma, H., Tsuji, H., Ishii, A., Watanabe, M., Takahashi, Y., Goto, J., Tsuji, S., and Akiyama, H. (2010) TDP-43 M337V mutation in familial amyotrophic lateral sclerosis in Japan. *Intern. Med.* **49,** 331–334
55. Tsai, C. P., Soong, B. W., Lin, K. P., Tu, P. H., Lin, J. L., and Lee, Y. C. (2011) FUS, TARDBP, and SOD1 mutations in a Taiwanese cohort with familial ALS. *Neurobiol. Aging* **32,** 553 e513–521
56. Yokoseki, A., Shiga, A., Tan, C. F., Tagawa, A., Kaneko, H., Koyama, A., Eguchi, H., Tsujino, A., Ikeuchi, T., Kakita, A., Okamoto, K., Nishizawa, M., Takahashi, H., and Onodera, O. (2008) TDP-43 mutation in familial amyotrophic lateral sclerosis. *Ann. Neurol.* **63,** 538–542
57. Del Bo, R., Ghezzi, S., Corti, S., Pandolfo, M., Ranieri, M., Santoro, D., Ghione, I., Prelle, A., Orsetti, V., Mancuso, M., Sorarù, G., Briani, C., Angelini, C., Siciliano, G., Bresolin, N., and Comi, G. P. (2009) TARDBP (TDP-43) sequence analysis in patients with familial and sporadic ALS. Identification of two novel mutations. *Eur. J. Neurol.* **16,** 727–732
58. Kühnlein, P., Sperfeld, A. D., Vanmassenhove, B., Van Deerlin, V., Lee, V. M., Trojanowski, J. Q., Kretzschmar, H. A., Ludolph, A. C., and Neumann, M. (2008) Two German kindreds with familial amyotrophic lateral sclerosis due to TARDBP mutations. *Arch. Neurol.* **65,** 1185–1189
59. Kamada, M., Maruyama, H., Tanaka, E., Morino, H., Wate, R., Ito, H., Kusaka, H., Kawano, Y., Miki, T., Nodera, H., Izumi, Y., Kaji, R., and Kawakami, H. (2009) Screening for TARDBP mutations in Japanese familial amyotrophic lateral sclerosis. *J. Neurol. Sci.* **284,** 69–71
60. Origone, P., Caponnetto, C., Bandettini Di Poggio, M., Ghiglione, E., Bellone, E., Ferrandes, G., Mancardi, G. L., and Mandich, P. (2010) Enlarging clinical spectrum of FALS with TARDBP gene mutations. S393L variant in an Italian family showing phenotypic variability and relevance for genetic counseling. *Amyotroph. Lateral Scler.* **11,** 223–227